Microelectronics Reliability 52 (2012) 933–936

Contents lists available at SciVerse ScienceDirect

Microelectronics Reliability

journal homepage: www.elsevier.com/locate/microrel

Improvement of lumen efficiency in white light-emitting diodes with air-gap embedded package

H.C. Chen [a], K.J. Chen [a], C.C. Lin [b], C.H. Wang [a], C.C. Yeh [a], H.H. Tsai [a], M.H. Shih [c], H.C. Kuo [a,*]

[a] Department of Photonics & Institute of Electro-Optical Engineering, National Chiao Tung University, 1001 University Road, Hsinchu 30010, Taiwan
[b] Institute of Lighting and Energy Photonics, National Chiao Tung University, 301 Gaofa 3rd Road, Guiren Township, Tainan County 711, Taiwan
[c] Research Center for Applied Sciences, Academia Sinica, Nankang, Taipei 115, Taiwan

ARTICLE INFO

Article history:
Received 10 January 2011
Received in revised form 3 February 2012
Accepted 16 February 2012

ABSTRACT

In this paper, white light-emitting diodes (LEDs) with air-gap embedded package were proposed and fabricated by a simple method including pulsed spray coating. The lumen efficiency of air-gap embedded LED was enhanced by 8.8% at driving current of 350 mA, compared to conventional remote phosphor white LED. This improvement was due to the enhanced utilization of blue and yellow rays, which were confirmed by pulse current-dependent correlated color temperature (CCT). The utilization efficiency of blue rays was enhanced by 12.4% due to the embedded air-gap layer. The simulation results performed by Monte-Carlo ray tracing method agreed with our experiments, which showed enhancement in lumen efficiency and similar CCT. Finally, the electric field intensity versus different thickness for air-gap and no air-gap embedded white LED was calculated to check the incident blue rays trapped in phosphor layer.

1. Introduction

Solid-state lightings, especially highly efficient white light-emitting diodes (LEDs), have been developed to replace traditional lighting source [1,2]. Generally, white light LEDs are fabricated by three methods: (1) individual red, green and blue LEDs mixing, (2) UV-LEDs exciting red, green and blue phosphors, (3) blue-LEDs converting yellow phosphors. The first two methods are not practical for high power white LEDs due to high cost and low conversion efficiency [3]. Therefore, the third method, also known as phosphor-converted LEDs (pcLEDs), has been widely deployed.

However, pcLEDs still have some imperfections and need to be optimized and improved, such as low conversion efficiency due to thermal issues [4] and limitation of extraction due to lead-frame package and silicone. One of the alternative methods is to move the phosphor layer away from the LED chip, known as remote phosphor LED, and by doing so, lumen efficiency of the white LED can be increased [5,6]. In all cases, one very important factor to be considered is the backscattering of the excited yellow photons. These yellow photons can only be collected when they are emitting towards the package top, and they are not very useful when they move towards the underneath chip surface [7]. Backscattering is not only unusable, but also causes reliability issues [5]. Consequently, an efficient extraction of backscattering light and improved extraction of light were very important. Previously, a scattered photon extraction (SPE) package which was developed by Narendran could enhance the extraction efficiency by 61% over that of conventional phosphor-converted white LED [7]. In addition, an inverted cone lens encapsulant and a surrounding ring remote phosphor layer were developed. This so-called ring remote phosphor structure could reduce the probability of the backward light from the phosphor layer to the absorptive LED chip [8].

In this paper, the lumen efficiency of remote phosphor white LEDs was further improved by embedding an air-gap layer in the LED package. By inserting a low-index layer under the phosphor layer, the downward light could be reflected. As a result, more blue rays and yellow rays could be extracted. Meanwhile, the air-gap structure can also trap the incident pumping blue rays inside to increase the absorption probability in phosphor layer and deliver more yellow rays than the conventional one-pass case. The experiment results showed improvements in lumen efficiency, compared to reference remote phosphor white LED. The behavior of light in such structure was investigated by simulation, and the calculation results showed the similar enhancement with our experiments.

2. Experiments

To form the air-gap structure, phosphor powder was first coated on an alternative substrate; here we use the polyethylene terephthalate (PET). Pulsed spray coating (PSC) was employed in this experiment to perform phosphor coating [9]. Phosphor powder (SrO_2–MgO–SiO_2–Eu_2O_3, silicate phosphor), silicone binder, and an alkyl-based solvent were mixed together to form phosphor suspension slurry. Then, the phosphor slurry with pulsing frequency of 5–10 Hz was sprayed onto the surface of bare PET, as shown

* Corresponding author. Tel.: +886 3 571 2121x31986; fax: +886 5 571 6631.
E-mail address: hckuo@faculty.nctu.edu.tw (H.C. Kuo).

0026-2714/$ - see front matter
http://dx.doi.org/10.1016/j.microrel.2012.02.011

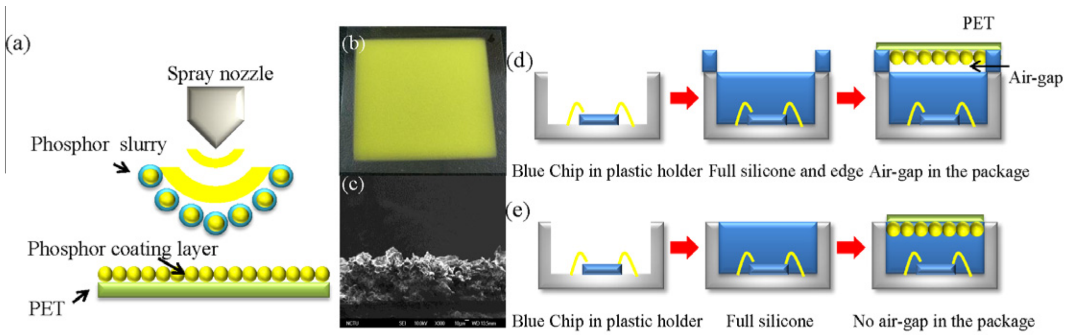

Fig. 1. (a) schematic diagram of the phosphor on the PET using PSC, (b) om image of the phosphor-coated PET, (c) the cross-sectional SEM image of phosphor layer on PET, (d) the process flow charts of air-gap embedded white LED and (e) conventional white LEDs.

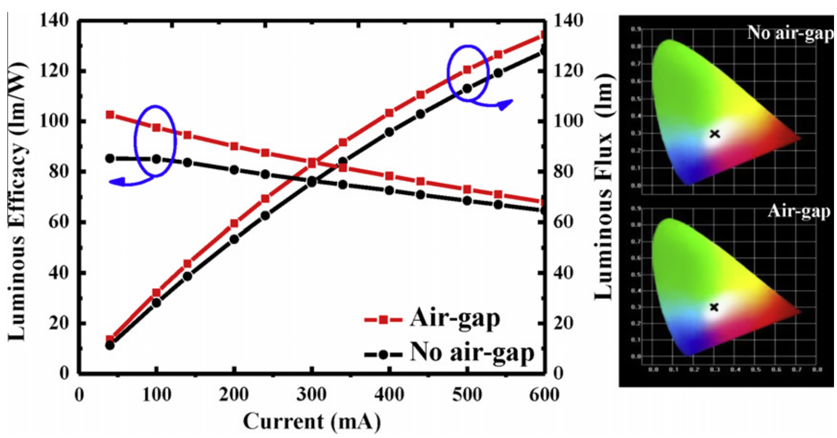

Fig. 2. The current-dependent luminous efficacies and the luminous fluxes of the air-gap embedded LED and the reference remote-phosphor LED at same color coordinate.

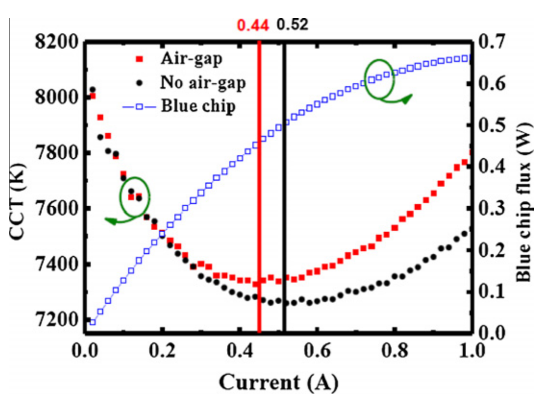

Fig. 3. Current-dependent CCT of the air-gap embedded white LED and the conventional white LED.

in Fig. 1a and b shows the top view of optical microscope (OM) of the phosphor-coated PET, and the phosphor was uniformly coated onto the surface of PET. The cross-sectional scanning electron microscope (SEM) image of phosphor layer was shown in Fig. 1c. The thickness and concentration of phosphor layer was about 100 μm and 50 wt.%, respectively. Fig. 1d shows the fabrication flow charts of the air-gap embedded white LED. First, the blue vertical LED with chip size of 1 × 1 mm^2 and emission wavelength of about 450 nm was placed in the commercial plastic lead-frame package by silver paste and wire-bonding. Then the silicone encapsulant was filled in the lead-frame. Third, the phosphor-coated PET was placed onto the lead-frame with silicone binder. For our conventional white LED, the silicone was entirely filled in the lead-frame, as shown in Fig. 1e. To form the air-gap layer, the silicone binder was placed only at the edge of lead-frame, so the phosphor layer would not directly contact with the underneath silicone. In order to mitigate the reduction of blue rays extraction due to insertion of air-gap, the silicone surface beneath air-gap was treated by dry etching. Finally, these samples were baked at 150 °C for one hour.

3. Results and discussion

Fig. 2 shows the current-dependent luminous efficacies and the luminous flux of the air-gap embedded white LED and the conventional remote phosphor white LED. The output power of our blue LEDs were about 380 mW at 350 mA. The measured luminous flux of air-gap and conventional white LEDs were 95.8 and 88 lm, respectively. By embedding an air-gap layer in remote phosphor white LED, the output lumen flux is enhanced by 8.8% and these two white LEDs exhibit almost the same CCT (7358 and 7325 K) and CIE coordinate. The improvement of lumen flux must be attributed to enhanced utilization of emission by both blue and yellow rays in the air-gap embedded structure.

Fig. 3 shows the CCT versus injection current of these two samples. In order to avoid the thermal effect on both LEDs and phosphor, the measurements were employed by pulse current source. First, for the conventional white LED, when the blue rays excited the phosphor, the yellow rays will emit in all directions. And the large part of downward rays, including blue and yellow rays, will

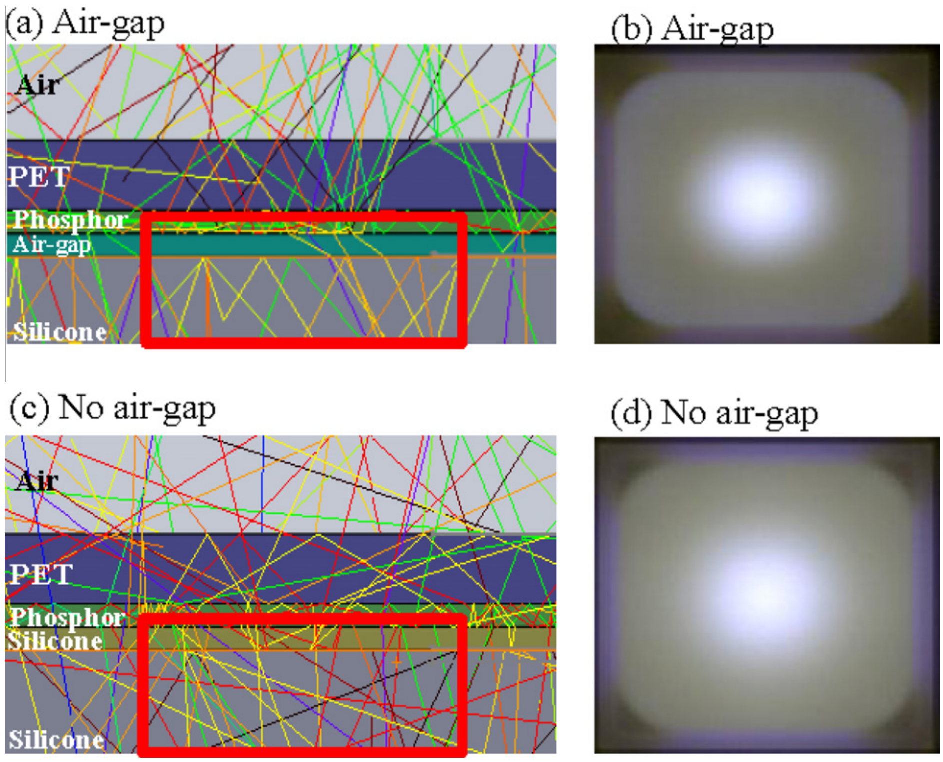

Fig. 4. (a) air-gap and (c) no air-gap embedded white LEDs, shows cross-section propagation of light in the package. The top view of lumen flux image (b) air-gap and (d) no air-gap embedded white LEDs.

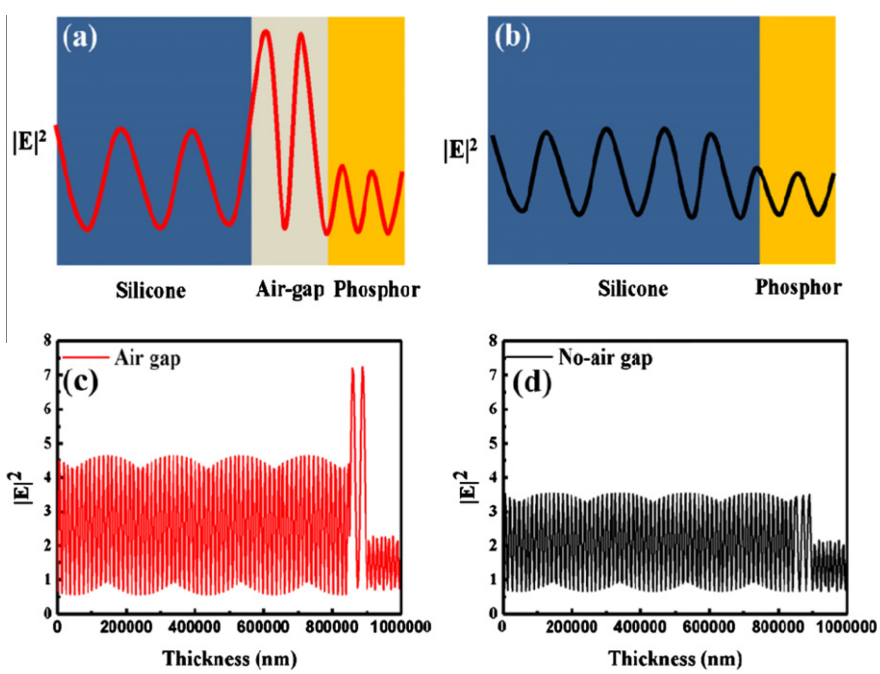

Fig. 5. Schematic diagram of thickness-dependent $|E|^2$ in (a) air-gap, (b) no air-gap embedded LEDs. Thickness-dependent $|E|^2$ of the (c) air-gap and (d) no air-gap embedded LEDs by TFCalc32 simulation.

transmit back to the blue LED chip, so the utilization of blue rays is low. And for the air-gap white LED, a significant portion of the downward rays would be reflected at air-phosphor layer interface. Instead of single pass, the blue photons can be reflected and go through phosphor again. However, the phosphor would not convert light with the same efficiency while too much blue light saturates the light conversion process. That's why the CCT of these two samples reduce first and then increase. The turning points of CCT were different for these two curves, the air-gap sample turns earlier than the conventional one, and the high current CCT is also higher in the air-gap sample than that in the conventional one. This phenomenon indicates that the utilization of blue rays in air-gap sample higher than that of the conventional white LED. Because the phosphor layer of these two samples had the same thickness and concentration, we could assume the saturation of blue rays intensities for these two samples were the same. The output power and saturation current of CCT for the air-gap embedded white LED and conventional white LED were 451 mW at 440 mA and 507 mW at 520 mA, respectively, as shown in Fig. 3. Then we can calculate the saturation intensity of these two samples by simple equation below:

$$I_{\text{air-gap saturation}} = I_{\text{no air-gap saturation}}$$
$$I_{\text{air-gap tunning point}} \times \eta_{\text{air}} = I_{\text{no air-gap tunning point}} \times \eta_{\text{no air}} \tag{1}$$

The I is the intensity of blue rays, and the η is the utilization of the blue rays in the package. By using the equation above, the utilization efficiency of blue rays in air-gap embedded white LED was enhanced by 12.4% compared to the conventional white LED.

Our designs were also modeled by using Monte-Carlo ray tracing simulation. The same intensity of blue rays into phosphor-layer is assumed in both cases. The detecting surface was placed into package, so it could collect the backscattered rays. The backscattering of air-gap embedded white LED was less than the conventional white LED, as shown in Fig. 4a–d shows the white light emission at the top surface of both LEDs. The lumen output of air-gap embedded white LED is enhanced by 13.7% and the CCT of these two LEDs are almost the same (7076 and 6991 K). The simulation results show that the backscattering was reduced and lumen flux was increased, which agree with our experiments.

One of the frequently asked questions about this air-gap structure is whether the introduction of air-gap will increase or decrease the actual blue photons coupling into the phosphor layer. To answer this, we need to resort to the optical multiple layer simulation. Therefore, we further simulate the electric field intensity versus different thickness for air-gap and no air-gap embedded white LEDs by TFCalc32 simulation, as shown in Fig. 5.

In this simulated condition, the air-gap was about 50 μm. Other conditions for silicone and phosphor layer were about 850 μm and 100 μm, respectively. Simultaneously, the 450 nm light was incidence into these layers by GaN LED. The power intensity of air-gap and no air-gap embedded white LEDs in phosphor layers can be calculated as follows:

$$W = \frac{\int_{850\mu m}^{900\mu m} n_p^2 \times |E|^2 dT}{\left[\int_{0\mu m}^{850\mu m} n_s^2 \times |E|^2 dT + \int_{850\mu m}^{900\mu m} n_a^2 \times |E|^2 dT + \int_{900\mu m}^{1000\mu m} n_p^2 \times |E|^2 dT\right]} \tag{2}$$

$$W = \frac{\int_{850\mu m}^{900\mu m} n_p^2 \times |E|^2 dT}{\left[\int_{0\mu m}^{850\mu m} n_s^2 \times |E|^2 dT + \int_{850\mu m}^{900\mu m} n_s^2 \times |E|^2 dT + \int_{900\mu m}^{1000\mu m} n_p^2 \times |E|^2 dT\right]} \tag{3}$$

where n_s, n_a, and n_p were the silicone, air, and phosphor refractive indexes, respectively and $|E|^2$ was the electric field intensity. According to the above Eqs. (2) and (3), the power intensity of the air-gap and no air-gap embedded white LEDs can be calculated, which were 9.3% and 7.5% at the wavelength of 450 nm. It is clear that the enhanced electric field intensity was occurred between air-gap and phosphor layers. The enhancement of power intensity can reach 24%, which leads to more blue rays trapped in air-gap layer. Meanwhile the absorption probability of phosphor can be enhanced. Therefore, more yellow rays could be produced due to this recycling of photons.

4. Conclusion

In summary, we proposed a method to enhance the lumen efficiency of remote phosphor white LED by embedding an air-gap layer. The fabrication process of air-gap embedded LED was very simple by employing PSC method. The enhancement of the lumen efficiency was due to the enhancement in utilization of blue rays from the LED, which was investigated by pulse current-dependent CCT. The utilization efficiency of blue rays of air-gap embedded white LED was enhanced by 12.4% compared to the conventional remote phosphor white LED, and the lumen efficiency was enhanced by 8.8% at driving current of 350 mA. Meanwhile, the simulation results demonstrate the backscattering of air-gap embedded white LED was less than the conventional white LED, the lumen output was enhanced by 13.7%, and the CCT of these two LEDs are similar, and all these calculation agree with our experiments.

Acknowledgments

The authors would like to thank Helio Opto., Kismart Corporation and Wellypower Optronics for their technical support. This work was funded by the National Science Council in Taiwan under Grant number NSC100-3113-E-009-001-CC2 and NSC-99-2120-M-009-007.

References

[1] Zhu Y, Narendran N. J Light Vis Environ 2008;32:2.
[2] Krames Michael R, Shchekin Oleg B, Mueller-Mach Regina, Mueller Gerd O, Zhou Ling, Harbers Gerard, et al. Disp Technol 2007;3(2).
[3] Kuo HC, Hung CW, Chen HC, Chen KJ, Wang CH, Sher CW, et al. Opt Express 2011;19:A930–6.
[4] Fan B, Wu H, Zhao Yu, Xian Y, Wang G. IEEE Photonic Tech L 2007;19(15).
[5] Narendran N, Gu Y, Freyssinier-Nova JP, Zhu Y. Phys State Solid 2005;202(6).
[6] Kim JK, Luo H, Schubert EF, Cho J, Sone C, Park Y, et al. J Appl Phys 2005;44(21):649–51.
[7] Narendran N. Proc SPIE 2005;5941:594108-1.
[8] Lin MT, Ying SP, Lin MY, Tai KY, Tai SC, Liu CH, et al. IEEE Photonic Tech L 2010;22:8.
[9] Huang HT, Tsai CC, Huang YP. Opt Express 2010;102:21.